Arabian Journal of Chemistry (2020) 13, 998–1010

King Saud University

Arabian Journal of Chemistry

www.ksu.edu.sa
www.sciencedirect.com

ORIGINAL ARTICLE

In vitro antitumor activity of water-soluble copper(I) complexes with diimine and monodentate phosphine ligands

Marina Porchia [a], Francesco Tisato [a], Mirella Zancato [b], Valentina Gandin [b,*], Cristina Marzano [b]

[a] *CNR-ICMATE, Corso Stati Uniti 4, 35127 Padova, Italy*
[b] *Department of Pharmaceutical and Pharmacological Sciences, University of Padova, via Marzolo 5, 35131 Padova, Italy*

Received 22 June 2017; accepted 6 September 2017
Available online 21 September 2017

KEYWORDS

Copper(I) complexes;
Antitumor activity;
Diimine ligands;
Phosphine ligands;
Water soluble

Abstract Copper(I) complexes including diimine ligands of the bicinchoninic acid (BCA) and bathocuproinedisulfonic acid (BCS) families and water-soluble phosphines have been synthetized, characterized and investigated for their in vitro anticancer potential against human tumor cell lines representing examples of lung, breast, pancreatic and colon cancers and melanoma. All copper complexes exhibited moderate to high cytotoxic activity and the ability to overcome cisplatin resistance. Remarkably, growth-inhibitory effects evaluated in human non-transformed cells revealed a preferential cytotoxicity versus neoplastic cells. The remarkable cytotoxic effect towards BxPC3 pancreatic cancer cells, notoriously poor sensitive to cisplatin, was not related to a DNA or proteasome damage.

1. Introduction

Platinum(II) drugs (*i.e.* cisplatin, carboplatin and oxaliplatin), although highly effective toward a number of solid tumors (Johnstone et al., 2016; Galluzzi et al., 2012; Kelland, 2007), are generally poorly selective towards cancer cells inducing severe toxic effects on healthy tissues as well as on cancerous ones. Moreover, this drawback is sometimes accompanied by the appearance of intrinsic or acquired resistance phenomena to the metallo-drug. For this reason, researches in the field of metal-based antitumor agents are still exploring other metals as potential source of novel drugs with improved pharmacological properties. Major efforts are devoted to the search of pharmacological targets alternative to DNA, the well-established Pt(II) target, and the challenge of metal complexes having physico-chemical properties different from those typical of Pt(II)-based drugs may help in this direction. Among several picks available in the transition metal group, copper is emerging as a potential alternative (Santini et al., 2014; Marzano et al., 2009; Tisato et al., 2010; Duncan and White,

* Corresponding author.
E-mail address: valentina.gandin@unipd.it (V. Gandin).
Peer review under responsibility of King Saud University.

Production and hosting by Elsevier

https://doi.org/10.1016/j.arabjc.2017.09.003
1878-5352

2012), according to the pronounced in vitro antitumor activity shown by properly designed copper complexes. Such an activity begins to be corroborated by favorable therapeutic profiles in some preclinical studies (Tisato et al., 2016; Gandin et al., 2014; Gandin et al., 2015). Different copper(I,II) complexes were reported to inhibit cancer growth in various experimental mouse tumor models, also including human tumor xenografts, without causing evident toxic or side effects. The low toxicity of antitumor copper complexes in healthy cells is likely due to intrinsic properties of copper. As an essential, endogenous metal in mammalian physiology, copper participates in several enzymes and proteins involved, for example, in energy metabolism and respiration. Hence, recognized as a non-toxic element at appropriate physiological concentrations, copper assembled in suitably tailored complexes may experience peculiar cell internalization and efflux processes in healthy cells, while maintaining cytotoxic efficacy in cancer cells, in which, due to the altered metabolism, copper accumulates at higher concentrations reaching 'toxic' levels.

Since the eighties, several copper compounds have been proposed as antitumor agents, some of them including N,N-diimine chelates and/or P-tertiary phosphine ligands (Santini et al., 2014; Marzano et al., 2009; Tisato et al., 2010). Diimines such as 1,10-phenantroline (phen) and 2,2′-bipyridine (bipy) or phosphines such as triphenylphosphine (PPh_3) and related bidentate bisaryldiphosphines (e.g. P-P = dppe: 1,2-bis(diphenylphosphino)ethane) allowed to synthetize quite lipophilic, cationic Cu(I) complexes of the type $[Cu(phen)_2]^+$, $[Cu(bipy)_2]^+$ and $[Cu(dppe)_2]^+$ with favorable in vitro cytotoxic properties (Santini et al., 2014; Marzano et al., 2009). The following transfer into in vivo tests revealed an unexpected cardiotoxicity in murine models (Hoke et al., 1989) that precluded clinical trials in humans. A possible explanation for the undesired outcome was the elevated lipophilicity of those cationic copper species that could drive cell internalization in cardiac cells and subsequent accumulation in the nucleus causing cardiotoxicity.

In agreement with the above experimental evidences, we and other authors thought to undertake the strategy of reducing the lipophilicity of the overall complex by introducing hydrophilic fragments in the coordination sphere of the metal. Ruiz-Azuara and co-workers designed a series of mixed $[Cu(II)(N\text{-}N)(AA)]^+$ compounds (N-N = di-imines of the phen and bipy family; AA = aminoacidate(1-)), then termed Casiopeinas® that indeed showed remarkable cytotoxic potency while decreasing the lipophilic character (Alemon-Medina et al., 2007). Our research group, instead, introduced water soluble phosphines in combination with N,N-chelates to generate mixed ligand complexes of the type $[Cu(I)(N\text{-}N)(PR_3)_2]$ (N-N = bis(pyrazolyl)borate(1-), bis(triazolyl)borate(1-) a PR_3 = (tris-hydroxymethyl)phosphine, 1,3,5-triaza-7-phosphaadamantane) (Porchia et al., 2013) confirming that reduction of the lipophilic character did not significantly affected the cytotoxic potency of the resulting complexes. Indeed, formation of homoleptic $[Cu(I)(PR_3)_4]^+$ compounds generated a class of hydrophilic molecules of remarkable cytotoxicity and unprecedented selectivity toward cancer cells (Tisato et al., 2016). On the contrary, ternary mixed-ligand complexes of the type $[Cu(I)(N\text{-}N)(PR_3)(X)]$ (N-N = phen and related diimine chelates, PR_3 = tris(cyanoethyl)phosphine, X = halide) (Gandin et al., 2013) with increased lipophilicity, while exhibiting cytotoxicity at nanomolar levels toward both sensitive and Pt-resistant cancer cells, also inhibited the growth of cultured non tumor cells. In parallel, fluorescence in situ hybridization (FISH) micronucleus assay attested high levels of genotoxicity in treated blood lymphocytes, thereby suggesting that the potential risk posed by di-imine metal complexes should be carefully reconsidered.

Trying to address the problems arose by the use of lipophilic copper(I) complexes as antitumor agents, we thought to synthetize a series of bis-substituted di-imine compounds along with two series of mixed di-imine/phosphine compounds (see Fig. 1), featuring complete solubility in water. Both hydrosoluble di-imines and phosphine ligands were employed, and the resulting complexes have been tested in vitro for their cytotoxic potential against several human tumor cell lines derived from solid tumors (including a cisplatin resistant subline) and towards human non tumor cells. An analysis of molecular and cellular pharmacology in human pancreatic BxPC3 cancer cells was performed in order to elucidate the role of di-imine and phosphine ligands in determining the biological properties of the related copper(I) complexes.

Both BCA and BCS diimine ligands were selected according to their recognized strong affinity for the Cu(I) ion, which allows the determination of complex formation constants of Cu(I) complexes in aqueous medium (Xiao et al., 2004) and serves as challenging probes for the determination of Cu(I) binding in proteins and peptides (Xiao et al., 2013). The versatility of these water-soluble diimines was also utilized to construct copper-based devices in material sciences for the application in dye-sensitized solar cells (Wills et al., 2013)

2. Results and discussion

2.1. Synthesis and characterization of copper(I) complexes 1–9

Copper complexes were synthesized via ligand-exchange reactions starting from the labile Cu(I) precursor $[Cu(CH_3CN)_4][BF_4]$. All of the complexes are deeply colored solid (from yellow to purple), stable in air and in solutions; they are soluble in water, methanol and acetonitrile exhibiting a solvatochromic behavior. A slightly modified synthesis of complex (**1**) has recently been reported in a nitrogen atmosphere, and the application of (**1**) in dye sensitized solar cells (DSSC) was described (Wills et al., 2013) The X-ray molecular structure of (**1**)-like evidenced that the two di-imines were virtually orthogonal adopting a pseudo tetrahedral geometry in the $[Cu(BCA)(H_2BCA)]^-$ anion, that was counterbalanced by a $[HEt_3N]^+$ cation, both features supporting the occurrence of a Cu(I) complex. Although there was no evidence of the $[PF_6]^-$ anion in the unit cell, characterization in solution by multinuclear ^{31}P and ^{19}F NMR spectroscopy and the detection of the peak at m/z 145 in the ESI(−) spectrum of the complex indicated the additional presence of one equivalent of co-crystallized $[HEt_3N][PF_6]$ (Wills et al., 2013).

During our syntheses we utilized more physiologically friendly Na^+ cations coming from di-imine ligands and $[BF_4]^-$ anions coming from the labile Cu(I) precursor. Also in our case, elemental analysis evidenced the presence of co-crystallized $NaBF_4$ in most compounds (complexes **1**,

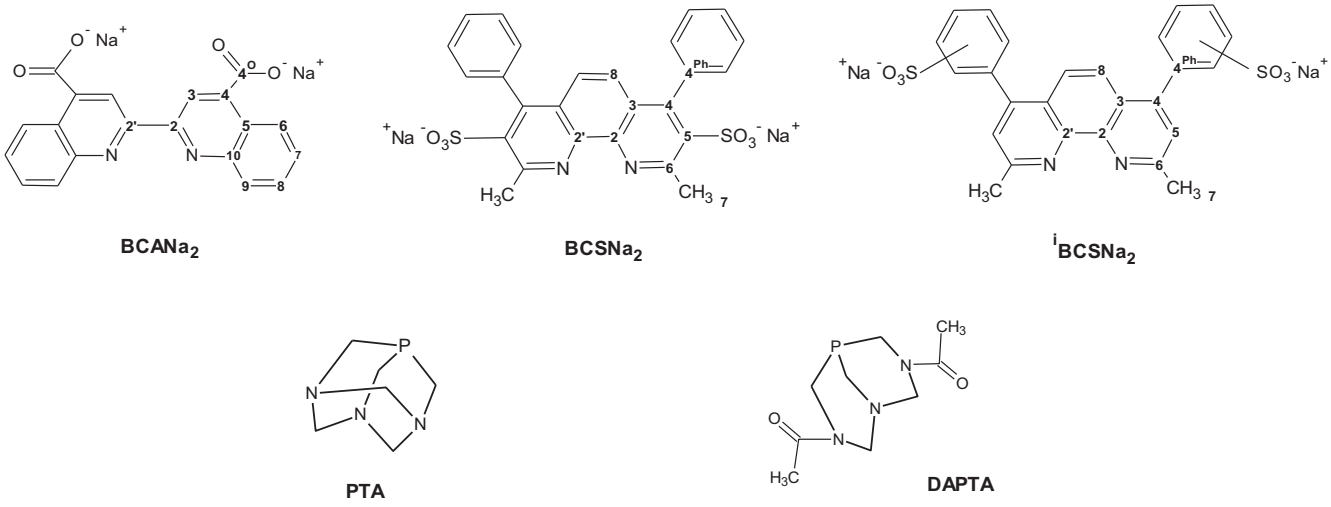

Fig. 1 Ligands utilised in the present study. $BCANa_2$ = 4,4′-dicarboxy-2,2′-biquinoline disodium salt (bichinconinic acid disodium salt); $BCSNa_2$ = bathocuproinedisulfonic acid disodium salt; $^{i}BCSNa_2$ bathocuproinedisulfonic acid disodium salt isomer mixture; PTA = 1,3,5-triaza-7-phosphaadamantane; DAPTA = 3,7-diacetyl-1,3,7-triazaphosphabicyclo[3.3.1]nonane.

4–**9**), in addition to the sodium atoms necessary to the overall charge balance of the complex. The presence of BF_4 was authenticated by detection of a broad band at ca. 1030 cm^{-1} in the pertinent IR spectra.

According to the characterization presented in the above reference study (Wills et al., 2013), our compounds were characterized by means of multinuclear ^{1}H, ^{13}C and ^{31}P NMR spectroscopy and electrospray ionization (ESI) mass spectrometry both in the positive and negative ion modalities. The easy collection of NMR spectra, typical of diamagnetic Cu(I) compounds, rules out metal oxidation phenomena occurring in solution in accordance with the presence of bulky di-imine ligands in homoleptic complexes **1**–**3**, and with the further presence of phosphines in mixed-ligand complexes **4**–**9**.

^{1}H and ^{13}C NMR spectra of bis-substituted di-imine complexes **1**–**3** were consistent with the proposed formulation. ^{31}P NMR spectra of mixed-compounds **4**–**9** showed each a distinctive singlet signal, downfield shifted and broadened, both features typical of copper coordination, compared to the signal of uncoordinated DAPTA or PTA phosphines (see Fig. 2).

For illustrative purposes, here follows the discussion of the NMR spectra of the mixed complex (**4**). Its ^{1}H spectrum shows a set of coupled aromatic protons in the 8.51–7.79 ppm range arising from the coordinated BCA framework (Fig. S1). Among these signals, the unique downfield shifted singlet corresponds to $H_{8,8'}$ (see Fig. 1 for proton caption). A further set of aliphatic signals in the 5.43–3.45 ppm range arises from the diastereotopic methylene protons of coordinated DAPTA. The coupling of diastereotopic protons of each methylene group is distinguishable in the ^{1}H-^{1}H COSY map of Fig. S2. Two further singlet signals at 1.91 and 1.77 ppm are due to magnetically unequivalent acetyl protons of DAPTA. Proton integrations indicate that coordination of the different ligands to the Cu(I) ion occurs in the 1:2 BCA:DAPTA ratio. The additional ^{1}H-^{13}C HMQC map allows the unequivocal assignment of ^{13}C signals from the relative ^{1}H-^{13}C coupling in accordance to the proton attribution (Fig. S3).

ESI-MS, in both positive and negative ion modalities, were utilized for the characterization of our Cu(I) complexes. ESI(−)MS was employed for homoleptic, bis-substituted compounds **1**–**3**, showing the molecular ion species at *m*/*z* 749 for $[Cu(HBCA)_2]^-$ and *m*/*z* 1101 for $[Cu(HBCS)_2]^-$. Bis-substituted species are detected together with mono-substituted adducts at *m*/*z* 405 ($[Cu(BCA)]^-$) and at *m*/*z* 581 ($[Cu(BCS)]^-$. Cleavages of CO_2 from the coordinated BCA and of SO_3 from coordinated BCS ligands were also detected.

For illustrative purposes, the ESI(−)MS behavior of complex (**2**) is below detailed. Full ESI(−) spectrum is outlined in Fig. 3, and the collisionally induced decomposition (CID) pathway is presented in Fig. 4 together with a pictorial sketch of fragmentation. The base peak in the full spectrum corresponds to the doubly charged $[(BCS)]^{2-}$ species at *m*/*z* 259, indicating that the complex is labile under ESI conditions. Significant peaks including copper are detected at *m*/*z* 1165 (10%), *m*/*z* 1101 (30%), *m*/*z* 581 (78%) and *m*/*z* 367 (30%). They correspond, respectively, to the ions [Cu(HBCS)(CuBCS)]$^-$, $[Cu(HBCS)_2]^-$ (molecular ion species), [Cu(BCS)]$^-$ and triply charged $[Cu(HBCS)_2]^{3-}$. CID of the molecular ion at *m*/*z* 1101 displays loss of a neutral di-imine with formation of the fragment ion at *m*/*z* 581([Cu(BCS)]$^-$), that, in turn, shows subsequent losses of SO_3 (−80 Da) and SO_2 (−64 Da) with formation of the fragment ion at *m*/*z* 501 and 437, respectively. As shown in Fig. 5, the attribution of the molecular ion species at *m*/*z* 1101 has been authenticated by comparison of the experimental and calculated cluster ion traces.

Considering mixed-ligand complexes **4**–**9**, ESI(+) spectra gave more informative results, whereas ESI(−) spectra did not show any ions including phosphines. Full ESI(+) spectra, while not showing the molecular ions $[Cu(diimine)(phosphine)_2]^+$, exhibited fragment ions of general formula $[Cu(diimine)(phosphine)]^+$ generated from the loss of a phosphine group. This behavior resembles that already observed for a family of similar $[Cu(N,N\text{-}\{CH_2(pz)_2\}(phosphine)_2]^+$ compounds, in which the molecular ion peak was never observed,

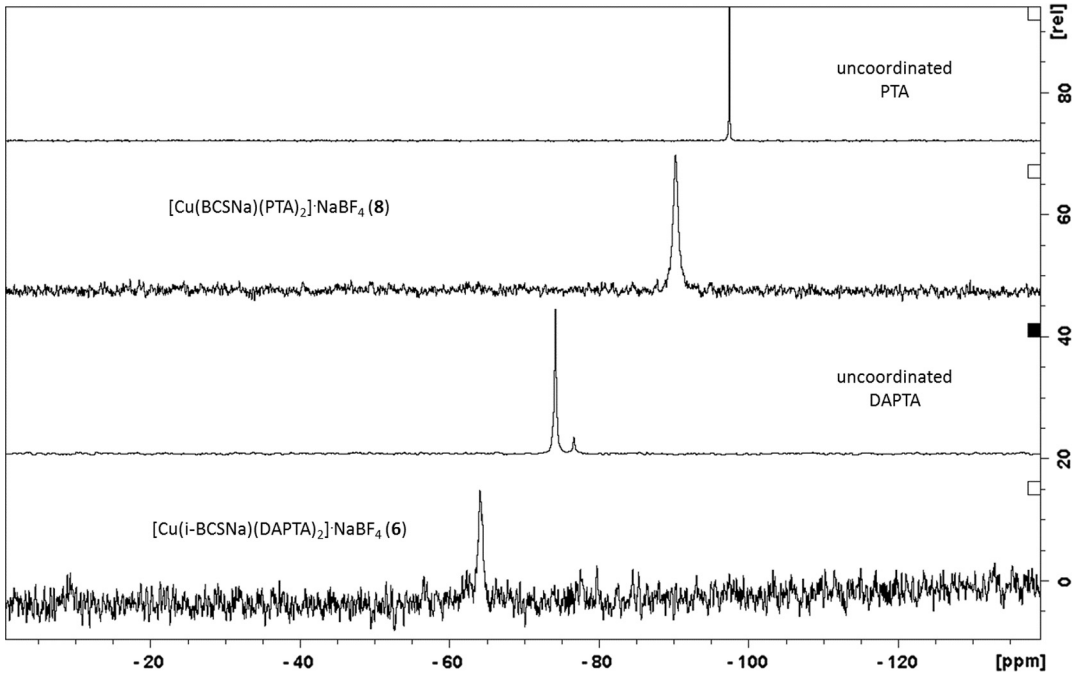

Fig. 2 Comparison of the ^{31}P NMR signals of uncoordinated PTA and DAPTA ligands with those arising from mixed-ligand complexes $[Cu(BCSNa)(PTA)_2]\cdot NaBF_4$ (**8**) and $[Cu(i\text{-}BCSNa)(DAPTA)_2]\cdot NaBF_4$ (**6**).

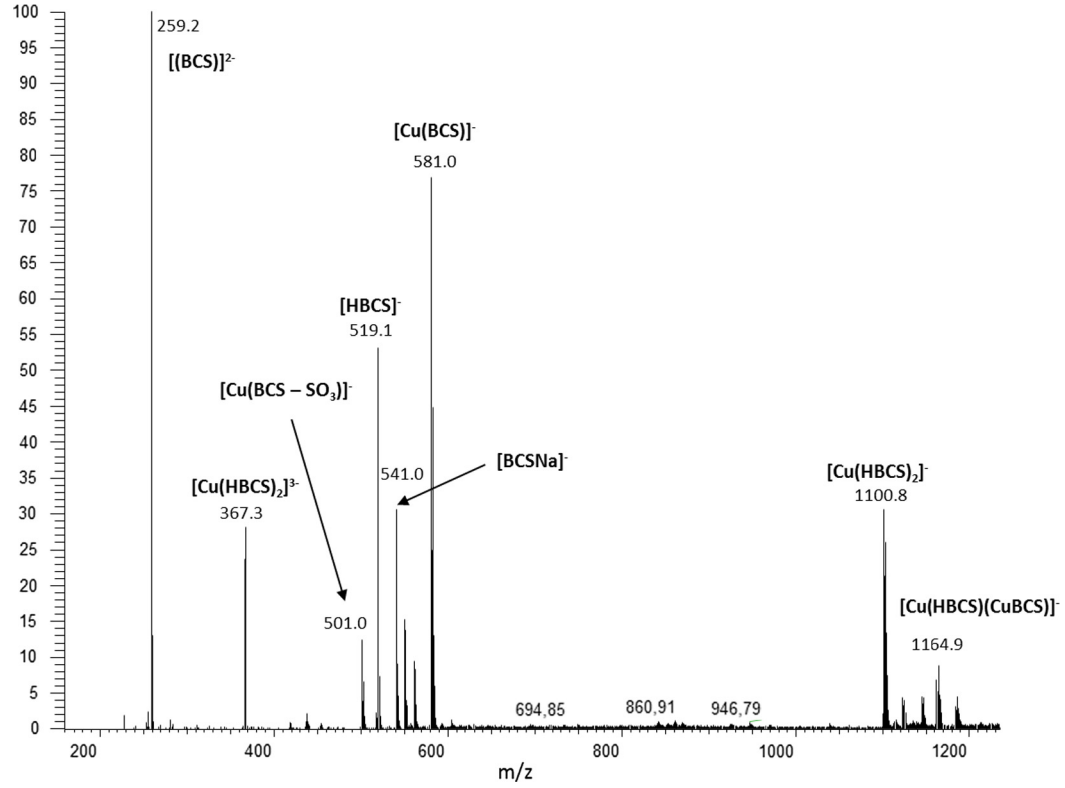

Fig. 3 Full ESI(−) spectrum of homoleptic, bis-diimine complex (**2**).

but the adduct $[Cu(N,N\text{-}\{CH_2(pz)_2\}(phosphine)]^+$ corresponding to the loss of one phosphine ligand were always detected (Porchia et al., 2013).

As an example of DAPTA derivatives, complex (**4**) displayed abundant $[Cu(H_2BCA)(DAPTA)]^+$ at m/z 636, $[Cu(HBCANa)(DAPTA)]^+$ at m/z 658 and $[Cu(BCANa_2)$

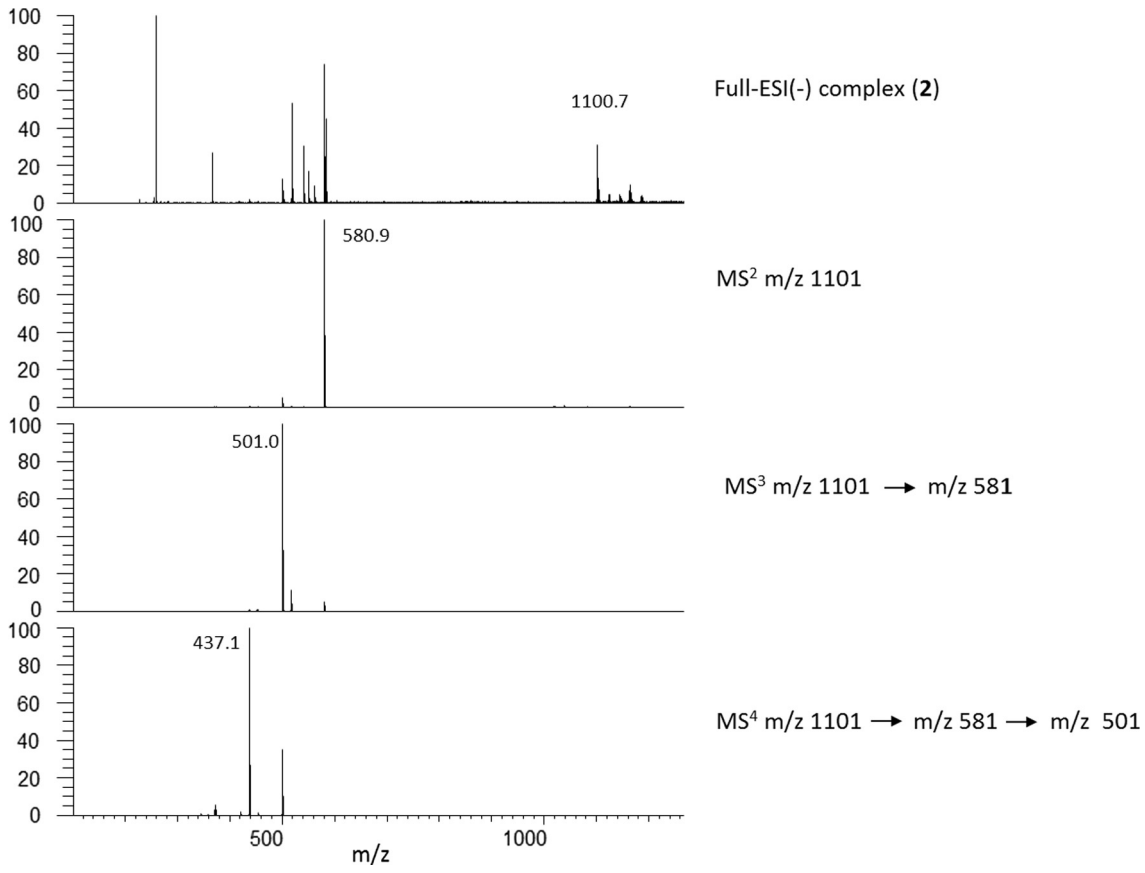

Fig. 4 Collisionally induced decomposition of the ion at *m*/*z* 1101 corresponding to the anion of complex (**2**).

$(DAPTA)]^+$ at *m*/*z* 680. These mixed species were flanked by low abundant rearranged ions $[Cu(DAPTA)_2]^+$ at *m*/*z* 521 and $[Cu(DAPTA)_3]^+$ at *m*/*z* 751, and by the metal free base peak $[(DAPTA)_2 + Na]^+$ at *m*/*z* 481 (Fig. S4). CID of the $[Cu(BCANa_2)(DAPTA)]^+$ ion at *m*/*z* 680 ion showed loss of DAPTA (−229 Da) followed by two subsequent losses of CO_2 with formation of the fragment ions at *m*/*z* 451, 407 and 363, respectively (Fig. S5). The latter fragmentation processes were accompanied by addition of water with formation of adducts at *m*/*z* 425 and 381, respectively.

Regarding PTA-containing mixed compounds **7**–**9**, the predominant peak in the ESI(+) full spectrum of complex **7** was due to the rearranged ion $[Cu(PTA)_2]^+$ at *m*/*z* 377, flanked by low abundant $[Cu(PTA)_3]^+$ at *m*/*z* 533 (25%) and $[Cu(BCANa_2)(PTA)]^+$ at *m*/*z* 608 (10%). As previously mentioned, ESI(−) spectrum did not show any peak containing PTA, but formation of clusters including BCA and their fragments due to loss of CO_2. Protonated, sodiated and cuprated $[Cu(BCA)]_2^{2-}$ dimer gave abundant ions at *m*/*z* 810, 833 and 874, respectively. The ESI(+) spectrum of complex (**7**) and the MS^n fragmentation of $[Cu(H_2BCA)(PTA)]^+$ at *m*/*z* 564 (Fig. S6) displayed similar profiles to those described for complex **4.**

Compounds **8** and **9** showed almost identical ESI(+) spectra giving the base peak at *m*/*z* 785 corresponding to $[Cu(BCSNa_2)(PTA)]^+$, with low abundant $[Cu(PTA)_2]^+$ at *m*/*z* 377 (10% for **8** and 35% for **9**). As observed in the spectra of complexes **2** and **3**, the ESI(−) traces of complexes **8** and **9** showed abundant peaks corresponding to $[Cu(BCS)]^-$ and $[Cu(i\text{-}BCS)]^-$ at *m*/*z* 581 due to loss of PTA ligands, and different sodiated and cuprated adducts at *m*/*z* 1165, 1187 and 1227, corresponding to $[Cu(HBCS)(BCSCu)]^-$, $[Cu(BCSNa)(BCSCu)]^-$ and $[Cu(BCSCu)(BCSCu)]^-$, respectively (see Fig. S7 for complex **8**).

2.2. Cytotoxicity

The in vitro antitumor activity of the newly synthesized copper (I) complexes (**1**–**9**) and of the corresponding uncoordinated ligands (PTA, DAPTA, $BCANa_2$, $BCSNa_2$ and i-$BCSNa_2$) were evaluated against a panel of human tumor cell lines derived from solid tumors. The cytotoxicity parameters, in terms of IC_{50} (the median growth inhibitory concentration calculated from dose–survival curves) obtained after 72 h exposure, are listed in Table 1. Cell lines representative of lung (A549), colon (HCT-15), breast (MCF-7) and pancreatic (BxPC3) cancers, along with melanoma (A375), have been included. For comparison purposes, cytotoxicity of cisplatin, the most widely used metal-based anticancer drug, was assessed under the same experimental conditions.

Cancer cell lines included in the screen were endowed with different degrees of sensitivity to cisplatin and showed a consistently good response to treatment with all tested compounds (concentration- and time-dependent antiproliferative profiles, data not shown), except the uncoordinated PTA ligand, which proved to be ineffective. Also the other uncoordinated di-imine and phosphine ligands, $BCANa_2$, $BCSNa_2$ and i-$BCSNa_2$ and

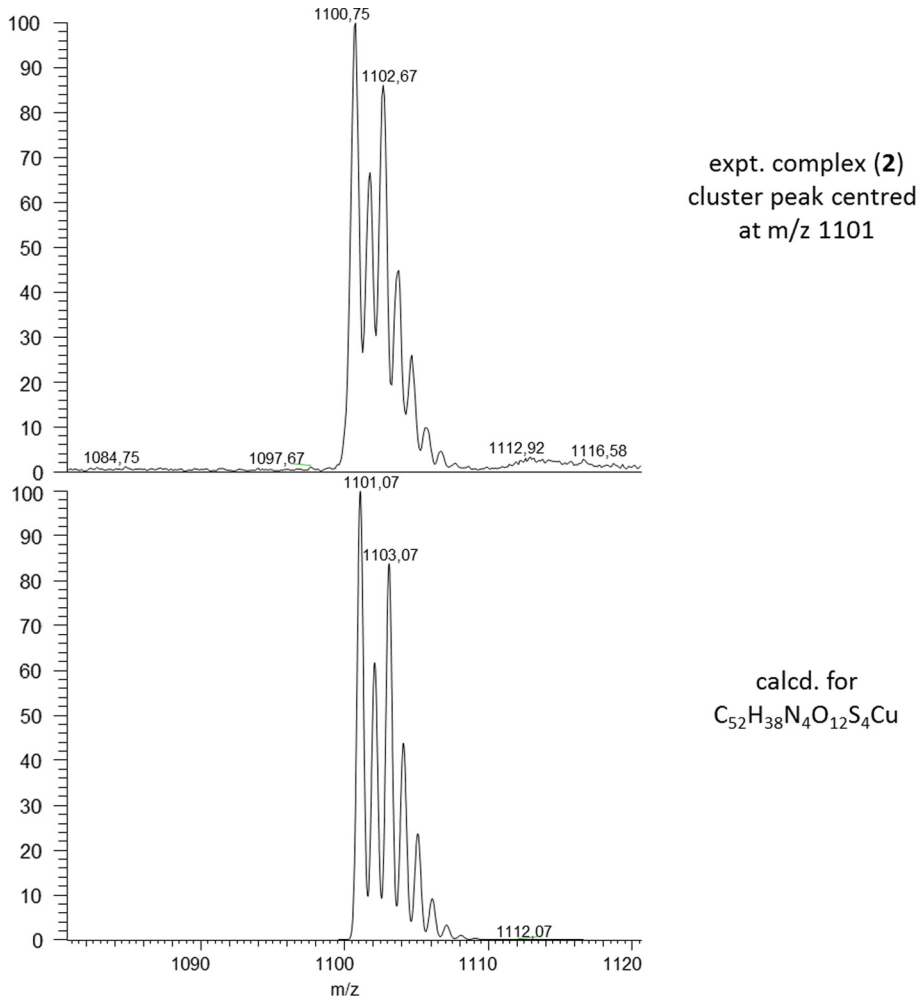

Fig. 5 Comparison of the experimental and calculated clusters of the ion at m/z 1101 corresponding to the anion of complex (**2**).

Table 1 In vitro antitumor activity.

Compound	IC_{50} (μM) ± D.S.				
	MCF-7	HCT-15	A375	BxPC3	A549
$[Cu(BCA)_2Na_3]\cdot NaBF_4$ (1)	9.22 ± 1.7	8.76 ± 2.3	11.78 ± 1.5	1.93 ± 0.4	6.25 ± 1.1
$[Cu(BCS)_2Na_3]$ (2)	21.51 ± 1.9	19.05 ± 1.8	16.55 ± 2.2	10.25 ± 1.4	26.5 ± 3.8
$[Cu(i\text{-}BCS)_2Na_3]$ (3)	41.58 ± 5.7	31.05 ± 3.6	42.58 ± 3.2	27.66 ± 3.2	34.51 ± 5.5
$[Cu(BCA)Na(DAPTA)_2]\cdot NaBF_4$ (4)	13.52 ± 1.9	10.54 ± 1.5	17.83 ± 2.8	7.25 ± 1.1	13.69 ± 2.2
$[Cu(BCS)Na(DAPTA)_2]\cdot NaBF_4$ (5)	5.76 ± 1.1	7.41 ± 1.1	17.63 ± 2.3	8.25 ± 1.2	13.52 ± 1.6
$[Cu(i\text{-}BCS)Na(DAPTA)_2]\cdot NaBF_4$ (6)	7.45 ± 1.2	7.36 ± 1.3	6.98 ± 1.1	2.1 ± 0.4	2.11 ± 0.3
$[Cu(BCA)Na(PTA)_2]\cdot NaBF_4$ (7)	12.26 ± 1.2	11.58 ± 1.6	15.42 ± 1.2	3.25 ± 0.5	7.5 ± 0.9
$[Cu(BCS)Na(PTA)_2]\cdot NaBF_4$ (8)	7.52 ± 1.7	6.25 ± 1.1	8.12 ± 1.3	1.58 ± 0.3	5.89 ± 1.4
$[Cu(i\text{-}BCS)Na(PTA)_2]\cdot Na_2BF_4$ (9)	7.53 ± 1.0	7.35 ± 1.1	9.51 ± 1.2	4.23 ± 0.2	1.26 ± 0.3
PTA	> 100	> 100	> 100	> 100	> 100
DAPTA	85.32 ± 3.95	67.12 ± 3.14	> 100	89.53 ± 4.13	> 100
$(BCA)Na_2$	69.62 ± 3.46	> 100	56.47 ± 3.14	> 100	> 100
$(BCS)Na_2$	> 100	> 100	54.25 ± 6.56	68.72 ± 3.12	> 100
$(i\text{-}BCS)Na_2$	> 100	> 100	67.64 ± 4.33	81.26 ± 4.50	> 100
***cis*platin**	7.60 ± 0.2	11.32 ± 1.5	3.36 ± 0.9	8.25 ± 1.7	10.56 ± 0.9

Cells ($3–8 \times 10^3$ mL^{-1}) were treated for 72 h with increasing concentrations of the tested compounds. The cytotoxicity was assessed by the MTT test. IC_{50} values were calculated by a four parameter logistic model, 4-PL ($P < 0.05$).

Table 2 Cross-resistance profile.

Compound	IC_{50} (μM) ± D.S.		
	2008	C13*	R.F.
$[Cu(BCA)_2Na_3]\cdot NaBF_4$ (1)	7.82 ± 1.1	4.11 ± 1.3	0.5
$[Cu(BCS)_2Na_3]$ (2)	15.25 ± 2.1	10.52 ± 2.8	0.7
$[Cu(i\text{-}BCS)_2Na_3]$ (3)	21.98 ± 2.3	31.22 ± 2.5	1.4
$[Cu(BCA)Na(DAPTA)_2]\cdot NaBF_4$ (4)	6.22 ± 1.1	1.55 ± 0.5	0.3
$[Cu(BCS)Na(DAPTA)_2]\cdot NaBF_4$ (5)	2.44 ± 0.2	3.10 ± 0.5	1.7
$[Cu(i\text{-}BCS)Na(DAPTA)_2]\cdot NaBF_4$ (6)	3.62 ± 0.6	3.81 ± 0.3	1.3
$[Cu(BCA)Na(PTA)_2]\cdot NaBF_4$ (7)	2.65 ± 0.7	2.11 ± 0.3	0.8
$[Cu(BCS)Na(PTA)_2]\cdot NaBF_4$ (8)	1.08 ± 0.4	0.9 ± 0.73	0.8
$[Cu(i\text{-}BCS)Na(PTA)_2]\cdot Na_2BF_4$ (9)	5.98 ± 0.6	7.11 ± 0.5	1.2
***cis*platin**	2.28 ± 0.5	22.77 ± 2.6	10

Cells ($3–8 \times 10^3$ mL^{-1}) were treated for 72 h with increasing concentrations of the tested compounds. The cytotoxicity was assessed by the MTT test. IC_{50} values were calculated by a four parameter logistic model, 4-PL ($P < 0.05$). RF = IC_{50} resistant/IC_{50} parental cell line.

Table 3 Cytotoxic activity against HEK293 non-tumor cells.

Compound	IC_{50} (μM) ± D.S.		
	HEK293	SI	SI_{BxPC3}
$[Cu(BCA)_2Na_3]\cdot NaBF_4$ (1)	22.50 ± 8.88	2.9	11.7
$[Cu(BCS)_2Na_3]$ (2)	54.55 ± 6.74	2.9	5.3
$[Cu(i\text{-}BCS)_2Na_3]$ (3)	65.47 ± 4.37	1.9	2.4
$[Cu(BCA)Na(DAPTA)_2]\cdot NaBF_4$ (4)	31.88 ± 4.51	2.5	4.4
$[Cu(BCS)Na(DAPTA)_2]\cdot NaBF_4$ (5)	29.22 ± 5.85	2.7	3.5
$[Cu(i\text{-}BCS)Na(DAPTA)_2]\cdot NaBF_4$ (6)	21.89 ± 4.58	4.2	10.4
$[Cu(BCA)Na(PTA)_2]\cdot NaBF_4$ (7)	25.22 ± 3.35	2.5	7.8
$[Cu(BCS)Na(PTA)_2]\cdot NaBF_4$ (8)	21.15 ± 7.97	3.6	13.5
$[Cu(i\text{-}BCS)Na(PTA)_2]\cdot Na_2BF_4$ (9)	20.36 ± 3.74	3.4	4.8
***cis*platin**	19.25 ± 1.6	2.3	2.3

Cells (5×10^3 mL^{-1}) were treated for 72 h with increasing concentrations of the tested compounds. The cytotoxicity was assessed by the MTT test. IC_{50} values were calculated by a four parameter logistic model, 4-PL ($P < 0.05$). SI = IC_{50} (non-tumor cells)/mean IC_{50} (cancer cells), SI_{BxPC3} = IC_{50} (HEK293 cells)/mean IC_{50} (BxPC3 cells).

DAPTA proved to be scarcely effective in decreasing cancer cell viability (even if detectable, average IC_{50} values were always over 50 μM). It's worth noting that uncoordinated lipophilic diimines, such as bipy and phen, exhibit cytotoxic activities in some cases comparable with that shown by cisplatin, due to their interaction with DNA by aromatic π stacking (Gandin et al., 2013).

A different behavior can be evidenced between the homoleptic complexes **1**–**3** and the heteroleptic ones **4**–**9**, as the former displayed a lower in vitro antiproliferative activity. Among homoleptic di-imine compounds (**1**–**3**), complex **1**, bearing the BCA ligand, was the most interesting derivative, yielding average IC_{50} values very similar to those obtained with cisplatin (7.6 and 8.2 μM, respectively). Complexes **2** and **3** were about 2- and 5-fold less effective than **1**, respectively.

Instead, mixed-ligand compounds (**4**–**9**) were quite active and in particular complexes bearing BCS and i-BCS ligands showed a marked cytotoxic activity, with IC_{50} values in the low micromolar range, and slightly lower than those recorded with cisplatin.

Complex **6**, the mixed copper(I) complex bearing i-BCS and DAPTA ligands, was the most promising derivative (mean IC_{50} values being 5.2 and 8.2 μM for **6** and cisplatin, respectively). Against human BxPC3 pancreatic and A549 lung cancer cells, complex **6** was roughly 4- and 5-fold more effective than the reference drug. Similarly, complexes **8** and **9** showed average IC_{50} values toward the in-house cell panel of 5.8 and 5.9 μM, respectively. Noteworthy, BxPC3 pancreatic cancer cells were the most sensitive cell line to copper(I) complexes. In detail, complex **8** bearing BCS and PTA ligands was roughly 5 times more effective than cisplatin against human pancreatic BxPC3 cell, notoriously poor sensitive to cisplatin.

All copper derivatives have been additionally tested for their in vitro antitumor activity on two human cell line pairs which have been selected for sensitivity/resistance to cisplatin (ovarian cancer cells 2008/C13*). Cytotoxicity on sensitive and resistant cells was assessed after 72 h of drug treatment by an MTT test. Table 2 shows the cytotoxicity parameters, in terms of IC_{50} and the resistance factor (RF), the latter defined as the ratio between IC_{50} values calculated for resistant cells and those obtained with sensitive ones. All copper complexes exhibited a different cross-resistance profile than cisplatin. Actually, the RF values were from 6- to 33-fold lower than that of cisplatin, indicating the absence of cross-resistance phenomena. These results are consistent with the

hypothesis that copper species possess mechanism(s) of action different from that shown by platinum drugs.

The cytotoxicity of tested complexes was also evaluated against non-tumor cells in rapid proliferation, the human embryonic kidney HEK293 cells (Table 3). All copper(I) complexes elicited a cytotoxic activity similar or even lower than that recorded with cisplatin. Interestingly, the selectivity index values (SI = quotient of the average IC_{50} toward normal cells divided by the average IC_{50} for the malignant cells) calculated for almost all complexes (excluding derivative **3**) were higher than that calculated with cisplatin, thus attesting a preferential cytotoxicity of copper(I) complexes versus neoplastic cells. Among all in the series, the mixed copper di-imine/phosphine compounds $[Cu(BCS)(PTA)_2]Na_2BF_4$ (**8**) and $[Cu(i\text{-}BCS)(DAPTA)_2]Na_2BF_4$ (**6**) distinguished as those possessing the highest SI values.

In addition, **6** and **8** showed SI_{BxPC3} values up to 6 times higher than that calcolated with cisplatin, being the SI_{BxPC3} the quotient of the IC_{50} toward normal cells divided by the IC_{50} for the pancreatic BxPC3 cancer cells.

2.3. Cellular accumulation and partition coefficient

With the aim of identifying a possible correlation between cytotoxic activity and cellular accumulation, the cellular copper content was measured in BxPC3 cells treated for 24 or 36 h with equimolar concentrations (5 μM) of tested compounds. The cellular copper levels were quantified by means of GF-AAS analysis, and the results, expressed as ng Cu per 10^6 cells, are shown in Fig. 6.

Although to a different extent, homoleptic and heteroleptic BCS and BCA derivatives (**1**, **2**, **4**, **5**, **7** and **8**) accumulated in a time-dependent manner, whereas cells treated with i-BCS complexes (**3**, **6** and **9**) did not show a time-dependent increase in cellular copper content.

To appreciate whether a correlation between lipophilicity and cellular uptake exists, the octanol/water partition coefficients (log P values outlined in Fig. 7) were measured using the shake-flask method. Among investigated compounds, *i*-BCS-containing derivatives **3**, **6** and **9** showed the highest hydrophilic character (logP = −0.21, −0.34 and −0.19, respectively). Considering the effect of phosphine on the hydrophilic balance of the compounds, PTA-containing complexes **7**–**9** showed all an elevated hydrophilic character. A linear correlation between lipophilicity and cellular association has been evidenced in the case of mixed-ligand complexes **4**–**9** (Fig. S8).

Matching the cytotoxic activity with the cellular uptake, a correlation was evidenced in the case of homoleptic copper(I) complexes (**1**–**3**). In fact the cellular copper content of BxPC3 cells treated for 36 h with the most cytotoxic derivative **1** was significantly higher than that recorded with compounds **2** and **3**. On the contrary, in the case of mixed complexes (**4**–**9**) no direct correlation could be derived.

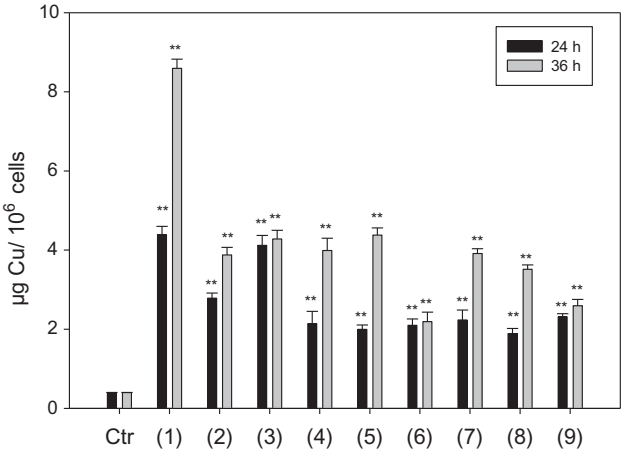

Fig. 6 Cellular uptake. Intracellular accumulation of copper complexes **1**–**9**. BxPC3 cells were incubated with 5 μM of copper complexes for 24 and 36 h, and cellular copper content was detected by GF-AAS analysis. Error bars indicate the standard deviation. $^{*}p < 0.05$; $^{**}p < 0.01$ compared with the control.

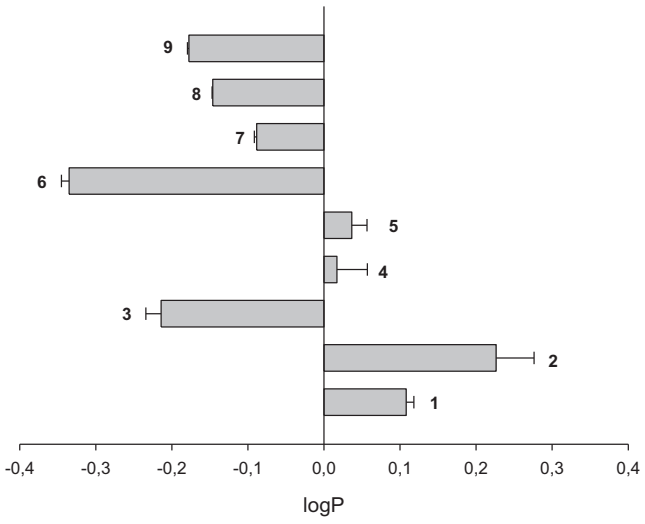

Fig. 7 Log P values (octanol/water) of complexes **1**–**9** obtained by shake flask method. Results are expressed as the mean ± SD of three independent experiments.

2.4. Effect of copper(I) complexes on ultrastructure morphology

It has been previously demonstrated that phosphino copper(I) complexes induce endoplasmic reticulum (ER) stress and trigger a nonapoptotic mechanism of programmed cell death (PCD), termed paraptosis (Gandin et al., 2012). On the contrary, mixed phosphino/di-imine derivatives induce apoptosis in different types of cancer cells (Gandin et al., 2013). In order to characterize the cellular morphological changes induced by the present copper(I) compounds, human pancreatic BxPC3 cancer cells were treated with complex **9** as representative of mixed-ligand compounds and analyzed by transmission electron microscopy (TEM) (Fig. 8). **9**-Treated BxPC3 cells showed the nucleus with a clearly defined ultrastructure, and regularly distributed chromatin. In addition, mitochondria appeared conserved in shape and internal structures, and no swelling features (increase in size and decrease in turbidity) could be detected. On the other hand, striking morphological changes, such as ER swelling and intracytoplasmic vacuoles, previously characterized as hallmarks of paraptotic cell death were distinctly noticed. Furthermore, **9**-treated cells stained

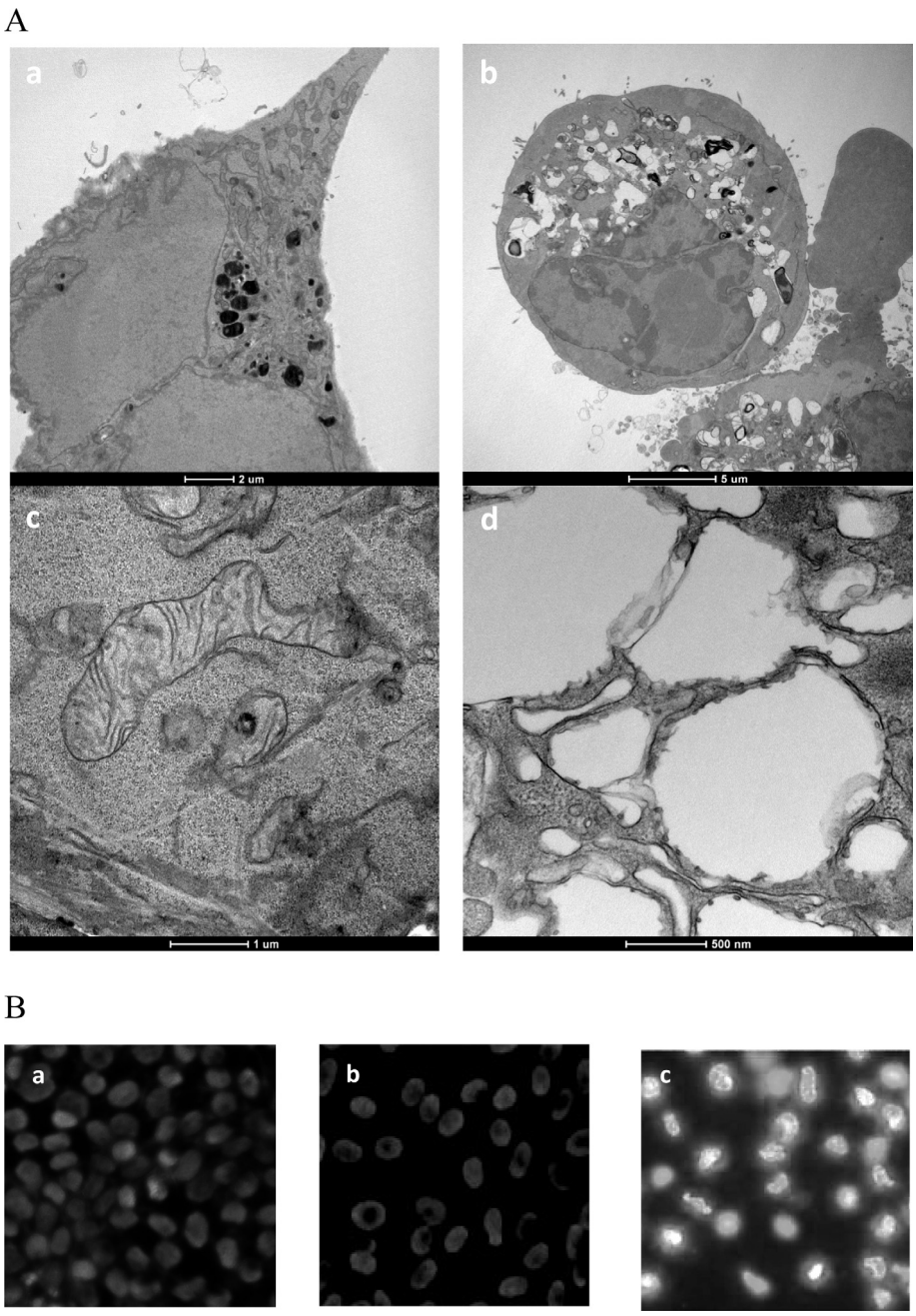

Fig. 8 Morphological changes. (A) Transmission electron micrographs of BxPC3 cells after 48 h of treatment with IC_{50} concentrations of compound **9**. (a) control cells; (b),(c), and (d) **9**. (B) Hoechst staining. BxPC3 cells were incubated for 48 h with IC_{50} of **9** (b) and cisplatin (c). Panel a represents the control untreated BxPC3 cells.

with Hoechst 33258 did not show nuclear DNA condensation or apoptotic body formation, classical hallmarks of apoptosis (Fig. 8, panel B).

Concerning the molecular basis underlying the mechanism of action of antiproliferative copper(I) complexes, some investigations recognized DNA (Gandin et al., 2013) or the proteasome multiprotein complex as the main molecular targets (Gandin et al., 2014; Gandin et al., 2012). On this basis, we evaluated the ability of complex **9** to interact with DNA in vitro by means of UV absorption titration and gel electrophoresis experiments. In addition, we assessed the ability of complex **9** to hamper proteasome proteolytic activities by testing chymotrypsin-like (CTL), trypsin-like (T-L) and caspase-like (C-L) activity of 26S proteasome isolated from rabbit. Neither DNA interaction nor proteasome inhibition were detected (data not shown), thus suggesting that its antiproliferative efficacy does not rely on DNA or proteasome targeting.

3. Conclusion

Copper(I) complexes including bis-substituted di-imines (**1** –**3**) along with two series of mixed di-imine/phosphine (**4** –**9**) featuring complete solubility in water were synthesized, characterized and tested in vitro for their cytotoxic potential against several cell lines derived from human solid tumors as well as towards human non-tumor cells. Differently from poorly cytotoxic free di-imines and phosphine ligands, all copper complexes exhibited moderate to high cytotoxic activity, and satisfactory selectivity toward human tumor cell lines. Moreover, these copper complexes overcame cisplatin resistance, and, in particular, all BCA-containing complexes **1**, **4** and **7** showed RF values <1 (till 33-fold lower than that of cisplatin), consistent with the hypothesis that copper compounds possess mechanism(s) of action different from platinum drugs, namely DNA damage. Neither DNA interaction nor proteasome inhibition were detected in pancreatic BxPC3 cancer cells, thus suggesting that the antiproliferative activity of this class of complexes does not rely on DNA or proteasome targeting.

As at present time there are no clear evidences of the mechanism(s) underlying the cytotoxic activity of this class of antiproliferative compounds, future studies are being scheduled. The detection of endoplasmic reticulum stress and intracytoplasmic vacuoles in **9**-treated BxPC3 cancer cells supports the hypothesis of the triggering of a programmed cell death (PCD) referred to as paraptosis, a PCD mechanism alternative to apoptosis already described for other antiproliferative copper compounds.

4. Materials and methods

4.1. Materials and general methods

Commercially available substances were of reagent grade and used without further purification. The reagents 4,4′-dicarboxy-2,2′-biquinoline disodium salt ($BCANa_2$), disodium 2,9-dimethyl-4,7-diphenyl-1,10-phenantrolinedisulfonate ($BCSNa_2$), bathocuproinedisulfonic acid disodium salt (i-$BCSNa_2$) and 5,6-diphenyl-3-(2-pyridyl)-1,2,4-triazine-4,4″-disulfonic acid sodium salt (ferrozine sodium salt, HFzNa) were obtained from commercial sources (Fluka, Sigma-Aldrich). The Cu(I) precursor $[Cu(CH_3CN)_4][BF_4]$ was prepared by reaction of $[Cu(H_2O)_6][BF_4]_2$ with metallic copper in acetonitrile. 1,3,5-triaza-7-phosphaadamantane (PTA), 3,7-diacetyl-1,3,7-triazaphosphabicyclo[3.3.1]nonane (DAPTA) and the homoleptic copper derivatives $[Cu(PTA)_4]BF_4$ (Porchia et al., 2009) and $[Cu(DAPTA)_4]BF_4$ (Gandin et al., 2015) were synthesized according to published methods. Elemental analyses were performed on a Carlo Erba 1106 Elemental Analyzer. ^1H, ^{31}P and ^{13}C NMR spectra were recorded on a Bruker AMX-300 instrument (300.13 MHz for ^1H, 75.47 MHz for ^{13}C and 121.41 MHz for ^{31}P), using $SiMe_4$ as internal reference (^1H and ^{13}C) and 85% aqueous H_3PO_4 as external reference (^{31}P). FT IR spectra were recorded on a Mattson 3030 Fourier transform spectrometer in the range 4000–400 cm^{-1} in KBr pellets. Mass spectra have been recorded by an electrospray LCQ ThermoFinnigan mass spectrometer. The purities of compounds used for biological activity determination, were checked by elemental analysis and were found to be ≥95%.

4.2. Synthesis and characterization of copper(I) complexes

4.2.1. Synthesis and characterization of bis-di-imino copper(I) complexes *1–3*

A general procedure was employed for the synthesis of copper complexes **1**–**3**, according to the procedure here detailed for **1**. An acetonitrile solution of $[Cu(CH_3CN)_4]BF_4$ (29 mg, 0.092 mmol) was added at room temperature to a stirring methanolic solution of the ligand 4,4′-dicarboxy-2,2′-biquinoline disodium salt ($BCANa_2$) (70 mg, 0.18 mmol) giving immediately a deep purple colour. The reaction mixture was stirred overnight, the volume of the solution was reduced under a nitrogen stream and diethyl ether was added. The mixture was filtered and the violet solid washed again with diethylether and dried under vacuum.

$[Cu(BCA)_2Na_3]\cdot NaBF_4$ (1) Dark purple solid. Yield: 47 mg; 55%. ^1H NMR (D_2O): δ (ppm) 8.76 (s, $H_{3,3'}$; 4H), 8.12 (d, $H_{9,9''}$; 4H), 7.72 (d, $H_{6,6'}$; 4H), 7.49 (t, $H_{7,7'}$; 4H), 7.25 (t, $H_{8,8'}$; 4H). $^{13}C\{^1H\}$ NMR (D_2O): δ (ppm) 174.7 (C-4^O; C═O), 152.5, 148.0, 145.8, 131.1 ($C_{7,7'}$), 129.0 ($C_{8,8'}$), 128.1 ($C_{6,6'}$), 125.8 ($C_{9,9'}$), 125.5, 116.4 ($C_{3,3'}$). IR (KBr, cm^{-1}): 3430 (br, s), 1606 (s), 1578 (s), 1559 (s), 1396 (m) 1385 (m), 1270(w), 1031 (br, m). ESI(−)MS in MeOH (m/z assignment, % intensity): 749 ($[Cu(HBCA)_2]^-$, 60), 659 ($[Cu(HBCA)_2$ – HCOOH - $CO_2]^-$, 15), 615 ($[Cu(HBCA)_2$ -2CO_2 - HCOOH$]^-$, 40), 571 ($[Cu(HBCA)_2$ -3CO_2 - HCOOH$]^-$, 100), 405 ([Cu(BCA)]$^-$, 25), 343 ([HBCA]$^-$, 70). Anal. Calcd. for $C_{40}H_{20}N_4O_8CuNa_4BF_4$: C 51.83, H 2.17, N 6.04. Found: C 52.11, H 2.54, N 5.80%.

$[Cu(BCS)_2Na_3]$ (2) Red solid. Yield: 74 mg; 65%. ^1H NMR (D_2O): δ (ppm) 7.90–7.22 (m, 24Har), 2.16 (bs, CH_3, 12H). $^{13}C\{^1H\}$ NMR (D_2O): δ (ppm) 157.4, 152.6, 147.6, 143.4, 137.2, 132.3, 129.5, 127.5, 126.0, 125.1, 123.2, 24.8 (CH_3). IR (KBr, cm^{-1}): 3432 (br, m), 1619 (m), 1190 (br, s), 1128 (m), 620 (m). ESI(−)MS in MeOH (m/z assignment, % intensity): 1165 ($[Cu(HBCS)(BCS) + Cu]^-$, 12), 1101 ($[Cu(HBCS)_2]^-$, 30), 581 ($[Cu(BCS)]^-$, 80), 541 ($[BCSNa]^-$, 30), 519 ($[HBCS]^-$, 55), 501 $[Cu(BCS - SO_3)]^-$, 15), 259 ($[BCS]^{2-}$, 100). Anal. Calcd. for $C_{52}H_{36}N_4O_{12}S_4CuNa_3\cdot 4H_2O$: C 50.30, H 3.57, N 4.51%. Found: C 50.34, H 3.70, N 4.79%.

$[Cu(i\text{-}BCS)_2Na_3]$ (3) Red solid. Yield: 64 mg; 60%. ^1H NMR (D_2O): δ (ppm) 7.81–7.20 (m, 24H), 2.08 (bs, CH_3, 12H). $^{13}C\{^1H\}$ NMR (D_2O): δ (ppm) 157.4, 147.6, 143.4, 137.0, 132.1, 129.4, 126.1, 125.9, 124.9, 123.1, 24.8 (CH_3). IR (KBr, cm^{-1}): 3461 (br, s), 1619 (m), 1196 br, s), 1128 (m), 620 (m). ESI(−)MS in MeOH (m/z assignment, % intensity): 1187 ($[Cu_2(i\text{-}BCS)_2 + Na^+]^-$, 10), 581 ($[Cu(i\text{-}BCS)]^-$, 20), 561 ($[Cu(i\text{-}BCS)_2 + Na^+]^{2-}$, 100). Anal. Calcd. for $C_{52}H_{36}N_4O_{12}S_4CuNa_3$: C 53.42, H 3.10, N 4.79%. Found: C 53.02, H 3.31, N 4.51%.

4.2.2. Synthesis and characterization of DAPTA di-imino copper(I) complexes *4–6*

A general procedure was employed for the synthesis of copper complexes **4**–**6**, according to the procedure here detailed for **4**. To an acetonitrile solution (10 mL) of $[Cu(CH_3CN)_4]BF_4$ (31 mg, 0.1 mmol) and DAPTA (46 mg, 0.2 mmol), a methanolic solution of the ligand 4,4′-dicarboxy-2,2′-biquinoline disodium salt ($BCANa_2$) (47 mg, 0.12 mmol) was added dropwise at room temperature. After 4 h, the volume of the solution was reduced to ca 2 mL under a dinitrogen stream

and diethyl ether was added. Leaving the mixture at 4 °C overnight a yellow solid was formed, which was collected by filtration, washed with chloroform and dried under vacuum.

[Cu(BCA)Na(DAPTA)$_2$]·NaBF$_4$ (4) Yellow solid. Yield: 69 mg; 68%. ^{1}H NMR (D_2O): δ (ppm) 8.51 (s, 2H, $H_{3,3'}$); 8.24 (dd, 4H, $H_{6,6';9,9'}$); 8.03 (t, 2H, $H_{7,7'}$); 7.79 (t, 2H, $H_{8,8'}$); 5.43 (d, 2H, H_{e2}); 5.02 (d, 2H, H_{d1}); 4.95 (d, 2H, H_{a1}); 4.50 (d, 2H, H_{d2}); 4.21 (d, 2H, H_{c1}); 3.93 (d, 2H, H_{e1}); 3.84 (d; 2H, H_{c2}); 3.58 (d, 4H, $H_{b1;b2}$); 3.45 (d, 2H, H_{a2}); 1.91 (s, 6H, CH_3); 1.77 (s, 6H, CH_3). ^{31}P{H} NMR (D_2O): δ (ppm) −63.5 (bs). ^{13}C{^{1}H} NMR (D_2O): δ (ppm) 20.43, 37.67, 42.56, 45.55, 61.38, 66.77 (sh 66.42), 116.47, 125.06, 126.82, 128.16, 129.59, 132.66, 146.37, 153.03, 172.26, 172.61, 173.79. ESI(+)MS in MeOH (m/z assignment, % intensity): 680 [Cu(BCA)Na$_2$(DAPTA)]$^+$, 25); 636 [Cu(BCA)Na$_2$(DAPTA) − CO_2]$^+$, 25); 521 ([Cu(DAPTA)$_2$]$^+$, 10); 481 ([(DAPTA)$_2$ + Na]$^+$, 252 ([DAPTA + Na]$^+$, 100). Anal.Calcd. for $C_{38}H_{42}CuN_8O_8P_2Na_2BF_4{\cdot}H_2O$: C 44.96, H 4.37, N 11.04%. Found: C 45.12, H 4.56, N 10.91%.

[Cu(BCS)Na(DAPTA)$_2$]·NaBF$_4$ (5) Yellow-brown solid. Yield: 87 mg; 74%. ^{1}H NMR (D_2O): δ (ppm) 7.85–7.14 (12H, $H_{Ar\text{-}BCS}$); 5.52 (d, 2H, H_{e2}); 4.98 (m, 4H, $H_{d1;a1}$); 4.57 (d, 2H, H_{d2}); 4.35 (d, 2H, H_{c1}); 4.05 (m, 4H, $H_{e1;c2}$); 3.67 (bs, 4H, $H_{b1;b2}$); 3.33 (d, 2H, $H_{a2;}$); 2.83 (s, 6H, C$H_{3Ar\text{-}BCS}$), 1.95 and 1.92 (s + s, 6 + 6H, 2-CH_{3DAPTA}). ^{31}P {H} NMR (D_2O): δ (ppm) −64.2 (bs). ESI(+)MS in MeOH (m/z assignment, % intensity): 856 ([Cu(BCS)Na$_2$(DAPTA)]$^+$, 15), 521 ([Cu(DAPTA)$_2$]$^+$, 10), 481 ([(DAPTA)$_2$ + Na]$^+$), 252 ([DAPTA + Na]$^+$, 100). ESI(−)MS in MeOH (m/z assignment, % intensity): 1165 ([Cu(BCS)]$_2$ + H]$^-$, 40), 1101 ([Cu(HBCS)$_2$]$^-$, 25), 581 ([Cu(BCS)]$^-$, 100), 519 ([HBCS]$^-$, 70), 259 ([BCS]$^{2-}$, 30). Anal. Calcd. for $C_{44}H_{50}CuN_8O_{10}P_2S_2Na_2BF_4$ C 45.04, H 4.30, N 9.55%. Found: C 44.79, H 4.79, N 9.89%.

[Cu(i-BCS)Na(DAPTA)$_2$]·NaBF$_4$ (6) Dark yellow solid. Yield: 84 mg; 72%. ^{1}H NMR (D_2O): δ (ppm) δ (ppm) 7.88–7.14 (12H, $H_{Ar\text{-}BCS}$); 5.52 (d, 2H, H_{e2}); 4.96 (m, 4H, $H_{d1;a1}$); 4.58 (d, 2H, H_{d2}); 4.37 (d, 2H, H_{c1}); 4.05 (m, 4H, $H_{e1;c2}$); 3.68 (bs, 4H, $H_{b1;b2}$); 3.29 (d, 2H, $H_{a2;}$); 2.80 (s, 6H, C$H_{3Ar\text{-}BCS}$), 1.96 and 1.93 (s + s, 6 + 6H, 2-CH_{3DAPTA}). ^{31}P{H} NMR (D_2O): δ (ppm) −64.1 (s). Anal. Calcd. for $C_{44}H_{50}CuN_8O_{10}P_2S_2Na_2BF_4$: C 45.04, H 4.30, N 9.55%. Found: C 45.34, H 4.46, N 9.74%.

4.2.3. Synthesis and characterization of PTA di-imino copper(I) complexes 7–9

A general procedure was employed for the synthesis of copper complexes **7**–**9**, according to the procedure here detailed for **7**. Phosphine ligand PTA (38 mg, 0.24 mmol) was added at room temperature to an acetonitrile solution of [Cu(CH$_3$CN)$_4$]BF$_4$ (37 mg, 0.12 mmol). After 10 min, to the clear reaction mixture a methanolic solution of the ligand 4,4′-dicarboxy-2,2′-biquino line disodium salt (BCANa$_2$) (47 mg, 0.12 mmol) was added dropwise giving rise to a deep orange colour. The reaction mixture was stirred overnight, the solvent was evaporated, the residue was dissolved in methanol and diethyl ether was added. An orange solid formed which was collected by filtration, washed with chloroform and dried under vacuum.

[Cu(BCA)Na(PTA)$_2$]·NaBF$_4$ (7) Orange solid. Yield: 46 mg; 45%. ^{1}H NMR (D_2O): δ (ppm) 8.50 (s, $H_{3,3'}$, 2H), 8.27 (d, $H_{9,9'}$, 2H), 8.17 (d, $H_{6,6'}$ 2H), 7.98 (t, $H_{7,7'}$, 2H), 7.78 (t, $H_{8,8'}$, 2H), 4.32 (bs, NCH_2N, 12H), 3.86 (bs, NCH_2P, 12H). ^{31}P{^{1}H} NMR (D_2O): δ (ppm) −89.0 (bs). ^{13}C NMR (D_2O): δ (ppm) 174.1 (C-4^O; C=O), 152.7, 149.4, 146.3, 132.3 (C_7), 129.4 (C_8), 128.3 (C_6), 126.5 (C_9), 124.8, 116.2 (C_3), 70.5 (s, N-CH$_2$), 48.2 (s, P-CH$_2$). IR (KBr, cm^{-1}): 3390 bm, 2939 m, 1608 s, 1581 s, 1400 bm, 1241 m, 1063 s, 1039 s, 1012 s, 968 s, 948 m. ESI(+)MS in MeOH (m/z assignment, % intensity): 608 ([Cu(BCA)Na$_2$(PTA)]$^+$, 10), 533 ([Cu(PTA)$_3$]$^+$, 25), 377 ([Cu(PTA)$_2$]$^+$, 100). ESI(−)MS in MeOH (m/z assignment, % intensity) 810 ({[Cu(BCA)]$_2$ + H$^+$}$^-$, 35), 404 ([Cu(BCA)]$^-$, 40), 360 ([Cu(BCA) − CO_2]$^-$, 15), 317 ([Cu(BCA) − 2 CO_2]$^-$, 100). Anal. Calcd. for $C_{32}H_{34}N_8O_4P_2CuNa_2BF_4{\cdot}2H_2O$: C 43.23, H 4.31, N 12.60. Found: C 43.06, H 4.97, N 12.64%.

[Cu(BCS)Na(PTA)$_2$]·NaBF$_4$ (8) Orange-red solid. Yield: 77 mg; 62%. ^{1}H NMR (D_2O): δ (ppm) 7.90–7.20 (12H, $H_{Ar\text{-}BCS}$), 4.39 (dd, NCH_2N, 12H), 3.87 (bs, NCH_2P, 12H), 2.74 and 2.66 (2s, 6 + 6H, 2-CH_3).

^{31}P{^{1}H} NMR (D_2O): δ (ppm) −90.2 (bs). ^{13}C{^{1}H} NMR (D_2O): δ (ppm), 158.5, 148.0, 147.3, 143.9, 138.3, 136.2, 132.4, 130.1, 129.6, 126.4, 125.9, 124.3, 70.6 (s, N-CH$_2$), 48.8 (s, P-CH$_2$), 26.9 (CH$_3$), 25.0 (CH$_3$). IR (KBr, cm^{-1}): 3407 bs, 1619 m, 1191 bs, 1126 m, 1035 s, 1012 m, 968 m, 948 m, 619 m. ESI(+)MS (m/z assignment, % intensity): 785 ([Cu(BCS)Na$_2$(PTA)]$^+$, 100), 627 ([Cu(BCS)Na$_2$]$^+$, 15).

ESI(−)MS: 1226 ({[Cu(BCS)]$_2$ + Cu$^+$}$^-$, 10), 1187 ({[Cu(BCS)]$_2$ + Na$^+$}$^-$, 15), 1165 ({[Cu(BCS)]$_2$ + H$^+$}$^-$, 5), 581 ({[Cu(BCS)]}$^-$, 60), 420 ({[Cu(BCS)] − 2SO$_3$}$^-$, 10), 259 ([BCS]$^{2-}$, 100). Anal. Calcd. for for $C_{38}H_{42}N_8O_6P_2S_2CuNa_2BF_4$4.5 H_2O: C 41.11, H 4.63, N 10.09%. Found C 41.31, H 4.80, N 9.94%.

[Cu(i-BCS)Na(PTA)$_2$]·NaBF$_4$ (9) Yellow solid. Yield: 95 mg; 71%. ^{1}H NMR (D_2O): δ (ppm) 7.94–6.84 (m, 12H), 4.40 (bs, NCH_2N, 12H), 3.89 (bs, NCH_2P, 12H), 2.65 and 2.60 (2s, 6H, 2-CH_3,). ^{31}P{^{1}H} NMR (D_2O): δ (ppm) −90.2 (s). ESI(+)-MS (m/z assignment, % intensity): 785 ({[Cu(BCS)Na$_2$(PTA)]}$^+$, 100), 377 ([Cu(PTA)$_2$]$^+$, 40), 158 ([PTA + H]$^+$, 10). ESI(−)MS: (m/z assignment, % intensity): 1165 ({[Cu(BCS)]$_2$ + H$^+$}$^-$, 30), 581 ([Cu(BCS)]$^-$, 100), 420 ({[Cu(BCS)] − 2SO$_3$}$^-$, 10), 259 ([BCS]$^{2-}$, 10). Anal. Calcd. for for $C_{38}H_{42}N_8O_6P_2S_2CuNa_2BF_4{\cdot}5H_2O$: C 40.78, H 4.68, N 10.89%. Found C 40.36, H 5.05, N 11.16%.

4.3. Experiments with cultured human cells

Copper complexes and the corresponding uncoordinated ligands were dissolved in deionized water. Cisplatin was dissolved in 0.9% sodium chloride solution. MTT (3-(4,5-dimethylthiazol-2-yl)-2,5-diphenyltetrazolium bromide), fluorogenic peptide proteasome substrates (N-Suc-Leu-Leu-Val-Tyr-7-amido-4-methylcoumarin (AMC), Boc-Gln-Ala-Arg-AMC, and Z-Leu-Leu-Glu-AMC), and cisplatin were obtained from Sigma Chemical Co, St. Louis, USA.

4.3.1. Cell cultures

Human lung (A549), breast (MCF-7), pancreatic (BxPC3), and colon (HCT-15) carcinoma cell lines along with melanoma (A375) were obtained from American Type Culture Collection (ATCC, Rockville, MD). Human embryonic kidney (HEK293) cells were obtained from European Collection of Cell Cultures (ECACC, Salisbury, UK). Human ovarian

cancer cell lines 2008 and its cisplatin resistant variant, C13*, were kindly provided by Prof. G. Marverti (Dept. of Biomedical Science of Modena University, Italy). Cell lines were maintained in the logarithmic phase at 37 °C in a 5% carbon dioxide atmosphere using the following culture media containing 10% fetal calf serum (Euroclone, Milan, Italy), antibiotics (50 units/mL penicillin and 50 μg/mL streptomycin), and 2 mM L-glutamine: (i) RPMI-1640 medium (Euroclone) for HCT-15, MCF-7, BxPC-3, 2008 and C13*; (ii) DMEM for A375 and HEK293 cells; (iii) F-12 HAM'S (Sigma Chemical Co.) for A549 cells.

4.3.2. MTT assay

The growth inhibitory effect toward tumor cells was evaluated by means of MTT assay. Briefly, $(3-8) \times 10^3$ cells/well, dependent upon the growth characteristics of the cell line, were seeded in 96-well microplates in growth medium (100 μL). After 24 h, the medium was removed and replaced with fresh media containing the compound to be studied at the appropriate concentration. Triplicate cultures were established for each treatment. After 72 h, each well was treated with 10 μL of a 5 mg/mL MTT saline solution, and following 5 h of incubation, 100 μL of a sodium dodecylsulfate (SDS) solution in HCl 0.01 M were added. After an overnight incubation, cell growth inhibition was detected by measuring the absorbance of each well at 570 nm using a Bio-Rad 680 microplate reader. Mean absorbance for each drug dose was expressed as a percentage of the control untreated well absorbance and plotted vs drug concentration. IC_{50} values, the drug concentrations that reduce the mean absorbance at 570 nm to 50% of those in the untreated control wells, were calculated by four parameter logistic (4-PL) model. All of the values are the means ± SD of not less than five measurements starting from three different cell cultures.

4.3.3. Cellular uptake

BxPC-3 cells (2×10^6) were seeded in 75 cm^2 flasks in growth medium (20 mL). After overnight incubation, the medium was replaced and the cells were treated with tested compounds for 24 or 36 h. Cell monolayers were washed twice with cold PBS, harvested and counted. Samples were than subjected to three freezing/thawing cycles at −80 °C, and then vigorously vortexed. The samples were treated with highly pure nitric acid (Cu: ≤ 0.005 μg kg^{-1}, TraceSELECT® Ultra, Sigma Chemical Co.) and transferred into a microwave teflon vessel. Subsequently, samples were submitted to standard procedures using a speed wave MWS-3 Berghof instrument (Eningen, Germany). After cooling, each mineralized sample was analyzed for platinum by using a Varian AA Duo graphite furnace atomic absorption spectrometer (Varian, Palo Alto, CA; USA) at the wavelength of 324 nm. The calibration curve was obtained using known concentrations of standard solutions purchased from Sigma Chemical Co.

4.3.4. Measurement of the partition coefficient

To determine the partition coefficient (P), the shake flask method was used. Octanol-saturated water (O) and water-saturated octanol (W) were prepared using analytical grade octanol and water. Compounds were first dissolved in DMSO and O and W mixing was done by vortexing for 30 min at room temperature to establish the partition equilibrium. Later, the two phases were by centrifugation at 3000*g* for 5 min and the copper content in each phase was determined by GF-AAS analyses. Partition coefficients of tested copper complexes were calculated using the equation log P = log ([Cu]W/[Cu]O).

4.3.5. Transmission electron microscopy

About 10^6 BxPC3 cells were seeded in 10 cm petri dishes. After 24 h the medium was removed and replaced with a fresh one containing the tested compound at the appropriate concentration.

Subsequently, the cells were washed in cold PBS, harvested and directly fixed in 1.5% glutaraldehyde buffered with 0.2 M sodium cacodylate, pH 7.4. After washing in the buffer and postfixation in 1% OsO4 in 0.2 M cacodylate buffer, specimens were dehydrated and embedded in epoxy resin (Epon Araldite). Sagittal serial sections (1 μm) were counterstained with toluidine blue. Thin sections (90 nm) were given a contrast by staining with uranyl acetate and lead citrate. Micrographs were taken with a Hitachi H-600 electron microscope (Hitachi, Tokyo, Japan) operating at 75 kV. All photos were typeset in Corel Draw 11.

4.3.6. Hoechst 33258 staining

BxPC3 cells (5×10^4) were seeded into 8-well tissue-culture slides (Sarstedt, Nümbrecht, Germany). After 24 h, cells were washed twice with PBS and following 48 h of treatment with IC_{50} concentration of tested complexes, cells were stained for 5 min with 1 mg/mL Hoechst 33258 (Sigma–Aldrich) in PBS before being examined by fluorescence microscopy (Olympus BX41, Cell F software, Olympus, Munster, Germany).

4.3.7. Statistical analysis

All of the values are the means ± SD of not less than three measurements starting from three different cell cultures. Multiple comparisons were made by ANOVA followed by the Tukey–Kramer multiple comparison test ($^{***}P < 0.001$; $^{**}P < 0.01$; $^{*}P < 0.05$), using GraphPad Software.

Acknowledgements

This work was financially supported by the University of Padova (Grants 60A04-0443, 60A04-3189 and 60A04-4015/15).

Appendix A. Supplementary material

Supplementary data associated with this article can be found, in the online version, at https://doi.org/10.1016/j.arabjc.2017.09.003.

References

Alemon-Medina, R., Brena-Valle, M., Munoz-Sanchez, J.L., Gracia-Mora, M.I., Ruiz-Azuara, L., 2007. Induction of oxidative damage by copper-based antineoplastic drugs (Casiopeinas). Cancer Chemother. Pharmacol. 60, 219–228.

Duncan, C., White, A.R., 2012. Copper complexes as therapeutic agents. Metallomics 4, 127–138.

Galluzzi, L., Senovilla, L., Vitale, I., Michels, J., Martins, I., Kepp, O., Castedo, M., Kroemer, G., 2012. Molecular mechanisms of cisplatin resistance. Oncogene 31, 1869–1883.

Gandin, V., Pellei, M., Tisato, F., Porchia, M., Santini, C., Marzano, C., 2012. A novel copper complex induces paraptosis in colon cancer cells via the activation of ER stress signalling. J. Cell Mol. Med. 16, 142–151.

Gandin, V., Porchia, M., Tisato, F., Zanella, A., Severin, E., Dolmella, A., Marzano, C., 2013. Novel mixed-ligand copper(I) complexes: role of diimine ligands on cytotoxicity and genotoxicity. J. Med. Chem. 56, 7416–7430.

Gandin, V., Tisato, F., Dolmella, A., Pellei, M., Santini, C., Giorgetti, M., Marzano, C., Porchia, M., 2014. In vitro and in vivo anticancer activity of copper(I) complexes with homoscorpionate tridentate tris(pyrazolyl)borate and auxiliary monodentate phosphine ligands. J. Med. Chem. 57, 4745–4760.

Gandin, V., Trenti, A., Porchia, M., Tisato, F., Giorgetti, M., Zanusso, I., Trevisi, L., Marzano, C., 2015. Homoleptic phosphino copper(I) complexes with in vitro and in vivo dual cytotoxic and anti-angiogenic activity. Metallomics 7, 1497–1507.

Hoke, G.D., Macia, R.A., Meunier, P.C., Bugelski, P.J., Mirabelli, C. K., Rush, G.F., Matthews, W.D., 1989. In vivo and in vitro cardiotoxicity of a gold-containing antineoplastic drug candidate in the rabbit. Toxicol. Appl. Pharmacol. 100, 293–306.

Johnstone, T.C., Suntharalingam, K., Lippard, S.J., 2016. The next generation of platinum drugs: targeted Pt(II) agents, nanoparticle delivery, and Pt(IV) prodrugs. Chem. Rev. 116, 3436–3486.

Kelland, L., 2007. The resurgence of platinum-based cancer chemotherapy. Nat. Rev. Cancer 7, 573–584.

Marzano, C., Pellei, M., Tisato, F., Santini, C., 2009. Copper complexes as anticancer agents. Anticancer Agents Med. Chem. 9, 185–211.

Porchia, M., Benetollo, F., Refosco, F., Tisato, F., Marzano, C., Gandin, V., 2009. Synthesis and structural characterization of copper(I) complexes bearing N-methyl-1,3,5-triaza-7-phosphaadamantane (mPTA): cytotoxic activity evaluation of a series of water soluble Cu(I) derivatives containing PTA, PTAH and mPTA ligands. J. Inorg. Biochem. 103, 1644–1651.

Porchia, M., Dolmella, A., Gandin, V., Marzano, C., Pellei, M., Peruzzo, V., Refosco, F., Santini, C., Tisato, F., 2013. Neutral and charged phosphine/scorpionate copper(I) complexes: effects of ligand assembly on their antiproliferative activity. Eur. J. Med. Chem. 59, 218–226.

Santini, C., Pellei, M., Gandin, V., Porchia, M., Tisato, F., Marzano, C., 2014. Advances in copper complexes as anticancer agents. Chem. Rev. 114, 815–862.

Tisato, F., Marzano, C., Porchia, M., Pellei, M., Santini, C., 2010. Copper in diseases and treatments, and copper-based anticancer strategies. Med. Res. Rev. 30, 708–749.

Tisato, F., Marzano, C., Peruzzo, V., Tegoni, M., Giorgetti, M., Damjanovic, M., Trapananti, A., Bagno, A., Santini, C., Pellei, M., Porchia, M., Gandin, V., 2016. Insights into the cytotoxic activity of the phosphane copper(I) complex [Cu(thp)4][PF6]. J. Inorg. Biochem. 165, 80–91.

Wills, K.A., Mandujano-Ramirez, H.J., Merino, G., Mattia, D., Hewat, T., Robertson, N., Oskam, G., Jones, M.D., Lewis, S.E., Cameron, P.J., 2013. Investigation of a copper(I) biquinoline complex for application in dye-sensitized solar cells. Rsc Adv. 3, 23361–23369.

Xiao, Z., Loughlin, F., George, G.N., Howlett, G.J., Wedd, A.G., 2004. C-terminal domain of the membrane copper transporter Ctr1 from Saccharomyces cerevisiae binds four Cu(I) ions as a cuprous-thiolate polynuclear cluster: sub-femtomolar Cu(I) affinity of three proteins involved in copper trafficking. J. Am. Chem. Soc. 126, 3081–3090.

Xiao, Z., Gottschlich, L., van der Meulen, R., Udagedara, S.R., Wedd, A.G., 2013. Evaluation of quantitative probes for weaker Cu(i) binding sites completes a set of four capable of detecting Cu(i) affinities from nanomolar to attomolar. Metallomics 5, 501–513.